

Koopman Methods for Estimation of Animal Motions over Unknown, Regularly Embedded Submanifolds

Nathan Powell, Bowei Liu, and Andrew J. Kurdila

Abstract—This paper introduces a data-dependent approximation of the forward kinematics map for certain types of animal motion models. It is assumed that motions are supported on a low-dimensional, unknown configuration manifold Q that is regularly embedded in high dimensional Euclidean space $X := \mathbb{R}^d$. This paper introduces a method to estimate forward kinematics from the unknown configuration submanifold Q to an n -dimensional Euclidean space $Y := \mathbb{R}^n$ of observations. A known reproducing kernel Hilbert space (RKHS) is defined over the ambient space X in terms of a known kernel function, and computations are performed using the known kernel defined on the ambient space X . Estimates are constructed using a certain data-dependent approximation of the Koopman operator defined in terms of the known kernel on X . However, the rate of convergence of approximations is studied in the space of restrictions to the unknown manifold Q . Strong rates of convergence are derived in terms of the fill distance of samples in the unknown configuration manifold, provided that a novel regularity result holds for the Koopman operator. Additionally, we show that the derived rates of convergence can be applied in some cases to estimates generated by the extended dynamic mode decomposition (EDMD) method. We illustrate characteristics of the estimates for simulated data as well as samples collected during motion capture experiments.

I. INTRODUCTION

A. The Problem Summary and the Estimation Problem

There are a wide variety of kinematic studies that evaluate animal motion [1], [2], [3]. Recent studies have focused on discovering fundamental principles of locomotion [4] and lower-dimensional representations of motion models across a vast number of different animals [5]. However, applying learning algorithms to kinematic models has been primarily reserved for human motion with prominent methods including [6], [7]. Recent learning methods have utilized neural networks and deep learning to synthesize and predict human motion [8], [9]. The time-dependent nature of these models has lead researchers to utilize recurrent neural networks (RNNs) in synthesize human motion [10], [11].

As powerful and promising as these methods are, none of these references study rates of convergence of estimates of animal motions. This paper extends our most recent work in [12]. In the paper [12], the authors explore methods to generate approximations of mappings over certain smooth manifolds in applications that estimate the motion of reptiles. The analysis determines error bounds for the estimation of functions over the motion manifolds. However, in [12] it is assumed that a known “template manifold” underlies a given motion regime. This paper seeks to generalize these results to the case when the underlying motion manifold is unknown.

In this paper, we assume that the motion of the animal is

governed by the uncertain equations

$$x_{i+1} = f(x_i), \quad (1)$$

$$y_{i+1} = G(x_{i+1}), \quad (2)$$

where $X := \mathbb{R}^d$ is the state space, $Y := \mathbb{R}^n$ is the output space, the function $f : X \rightarrow X$ that determines the dynamics is unknown, and the observable function $G : X \rightarrow Y$ is unknown. It is further assumed that this evolution law exhibits some additional “hidden” structure. Specifically, it is assumed that there is a compact, smooth Riemannian manifold Q that is regularly embedded in X that is invariant under the flow generated by Equation 1. The task is to collect finite samples $\{(x_{k_i}, y_{k_i})\}_{i=1}^M \in Z = X \times Y$ of state and output pairs at discrete times $\mathbb{T}_M := \{k_i \in \mathbb{N} \mid 1 \leq i \leq M\}$ and use them to build an estimate of the observable function G . Here \mathbb{N} is the collection of nonnegative integers. Is it possible to choose the k_i sequentially so that $k_1 = 1, k_2 = 2, \dots$ etc, but the approach in this paper does not require uniform sampling.

Examples 1 and 2 described below show that the model class described above is very rich: there are a wide variety of models of the form above that are obtained when geometric methods [13], [14] are discretized in time.

Example 1: This first example illustrates how quite general motion estimation problems of the type governed by Equation 1 may arise. For a wide variety of animal models, it is popular to create models that consist of rigid bodies connected by ideal joints. Such a model for human motion can be constructed by choosing as states the rigid body motion of a core body, spherical joints for the hips and shoulders, and revolute joints for all the remaining joints of the body. For human motion, the full configuration manifold might be taken as

$$\begin{aligned} \hat{X} := & \underbrace{SE(3) \times SO(3) \times S^1 \dots S^1}_{\text{core body}} \times \underbrace{SO(3) \times S^1 \dots S^1}_{\text{left arm}} \times \underbrace{SO(3) \times S^1 \dots S^1}_{\text{right arm}} \\ & \times \underbrace{SO(3) \times S^1 \dots S^1}_{\text{left leg}} \times \underbrace{SO(3) \times S^1 \dots S^1}_{\text{right leg}}. \end{aligned}$$

In the above expression $SE(3)$ and $SO(3)$ designates the special Euclidean group and special orthogonal group respectively in three dimensions. It is known by the Nash embedding theorem that $\hat{X} \subset X = \mathbb{R}^d$ for a d large enough. Standard geometric methods as in [13], [14] describe how equations of motion generate a flow $\{S(t)\}_{t \in \mathbb{R}^+}$ in continuous time over \hat{X} . By discretizing the flow at times $t_p := p\Delta$ with Δ a fixed time step, we obtain the evolution law $x_{p+1} = S(\Delta)x_p$. The discretization yields a discrete

dynamics of the form in Equation 1 with $f = S(\Delta) : \hat{X} \subset X \rightarrow \hat{X} \subset X$. If we suppose that the output space Y consists of the inertial positions of j distinguished points on the body, the kinematics map $G : \hat{X} \rightarrow \mathbb{R}^{3j} := Y$. In motion capture studies that seek to study certain motion regimes, it is then natural to hypothesize an existence of an unknown submanifold $Q \subseteq \hat{X} \subseteq X$. The estimation problem is then to use the measurements $\{(x_{k_i}, y_{k_i})\}_{i=1}^M$ to build approximations of $G : Q \rightarrow Y$, where manifold Q is unknown. The strategy in this paper can be realized, at least in principle, using RKH spaces with bases that are the tensor product of bases for functions over $SO(3)$ or other homogeneous manifolds. Such bases are studied, for example, in [15], [16].

Example 2: For this short paper, we perform numerical studies of some simpler problems that are common in animal motion. Instead of modeling or studying motions in the full configuration space above, it is often of interest to understand the motion for just an appendage, or across a joint. For simplicity, we carry out numerical studies in this paper when Q is a unknown Riemannian manifold Q that is regularly embedded in $X := \mathbb{R}^d$. Again, if we assume that Y is defined in terms of the inertial positions of j points on the body, we have $G : X \rightarrow Y$ with $Y := \mathbb{R}^{3j}$. The estimation task is to use samples $\{(x_{k_i}, y_{k_i})\}_{i=1}^M \subset X \times Y$ to build approximations of G , even though the manifold Q is unknown.

B. Overview of New Results

The analysis of the uncertain estimation problem in this paper is carried out using tools from Koopman theory. Koopman theory is a family of results that studies the behavior of dynamical systems in terms of operator theory, and it constitutes a powerful framework for studying nonlinear dynamics. Very recent accounts of the general theory can be found in book [17] or edited volume [18]. Of the hundreds of papers related to Koopman theory, some of the most relevant to this paper investigate approximations of the Koopman operator, which includes [19], [20], [21], [22], [23]. Also, the specific work in [19], [20] that describes the extended dynamic mode decomposition (EDMD) algorithm for the approximation of the Koopman operator is also quite relevant to this paper. Later in Section II-C a detailed description is given of the EDMD algorithm and how it is used to approximate the Koopman operator. For this introduction and description of contributions, it suffices to note that the Koopman operator U_f associated with the discrete Equation 1 is defined by the identity $U_f g = g \circ f$, with f the fixed function that appears in the unknown dynamics. References [24], [17], [19], [20], [21], [22], [23] give detailed accounts of how approximations of the Koopman operator U_f can be used in derivations of forecasting schemes or state estimators, estimation of observable functions, identification of nonlinear state equations, or in the approximation of Koopman modes, as well as other important estimation tasks.

To be precise about the contributions of this paper to the rapidly growing field of Koopman theory, we briefly

summarize the overall strategy taken in this paper. This overall strategy is common to many of the approaches outlined in References [24], [17], [19], [20], [21], [22], [23], but in this paper, we focus on determining how to ensure error bounds not found in these references. Since $Q \subset X$ is unknown, but the ambient space X is known, a kernel function $\mathfrak{K} : X \times X \rightarrow \mathbb{R}$ is selected that defines a reproducing kernel Hilbert space (RKHS) H of real-valued functions over the known set X . A kernel section, or kernel basis function, centered at a point $x \in X$ is defined in terms of the kernel as $\mathfrak{K}_x(\cdot) := \mathfrak{K}(x, \cdot)$. Finite dimensional spaces of approximants H_M are defined in terms of bases $\{\mathfrak{K}_{\xi_{M,i}}\}_{i=1}^M$ over the full set X , which depend on some set of samples $\Xi_M := \{\xi_{M,i} := x_{k_i} \mid 1 \leq i \leq M\}$ collected along trajectories of the uncertain system at the discrete times $\mathbb{T}_M := \{k_i \mid 1 \leq i \leq M\}$. Hence, we have the spaces of approximants $H_M := \text{span}\{\mathfrak{K}_{\xi_{M,i}} \mid \xi_{M,i} \in \Xi_M\}$. Approximations of the observable function G for the uncertain system are built using the finite dimensional spaces H_M and the H -orthogonal projection $\Pi_M : H \rightarrow H_M$. Data-dependent approximations U_f^M of the Koopman operator U_f are defined by the identity $U_f^M g := \Pi_M((\Pi_M g) \circ f)$, which has a coordinate representation shown in Equation 9. By inspection of the coordinate expression, it is clear that the approximation U_f^M of the Koopman operator U_f can be constructed from the samples $\{(x_{k_i}, y_{k_i})\}_{i=1}^M$ and the choice of finite dimensional space H_M . This paper introduces an approximation method in which the distribution of the samples $\{x_{k_i}\}_{i=1}^M$, the definition of the space H_M , and the choice of the kernel \mathfrak{K} determines the rate of convergence of $U_f^M g \rightarrow U_f g$.

There are three distinct contributions in this paper to the state-of-the-art in estimation methods for the system in Equations 1 and 2.

(1) *Reduced Order Models of Animal Motion:* Although Koopman methods have been studied for a wide variety of application areas, this paper is the first systematic study of the method for characterizing animal motions over submanifolds. The approach should be of general interest to those studying reduced order models of animal motions. The paper describes a rigorous formulation of a general method for approximating such motions, and the theory includes estimates of the rates of convergence in various function spaces as the number of samples M increases. Such estimates are not available in the literature on motion estimation such as in [6], [7], [9], [8], [10], [11].

(2) *Convergence Rates for Koopman Approximations:* In addition, this paper describes general, strong rates of convergence of data-dependent approximations of the Koopman operator. This result is of interest in its own right. Full details on the derivation and interpretation of these rates is given in the discussion of Theorem 2 below, but we briefly summarize the structure and novelty of these rates here. The primary result of this paper defines a regularity assumption in the framework of Koopman theory that is particularly powerful and enables determination of strong error bounds.

The regularity assumption states that if the pullback space $f^*(H) := \{g : Q \rightarrow \mathbb{R} \mid g = h \circ f, h \in H\}$ is continuously embedded in a Sobolev space, then we get strong rates of convergence. These rates of approximation are bounded by $O(h_{\Xi_M, Q}^r)$ where $h_{\Xi_M, Q}$ is the fill distance of samples Ξ in the manifold Q , $h_{\Xi_M, Q} := \sup_{q \in Q} \inf_{\xi_{M,i} \in \Xi_M} d_Q(q, \xi_{M,i})$ where d_Q is the metric over Q and r is an index that measures smoothness in a Sobolev space. Thus, even though the manifold Q is unknown, we obtain a geometric characterization of the error. The convergence depends on how quickly samples fill up the unknown manifold. These rates for the Koopman approximation problem are qualitatively similar to rates of convergence that are familiar in regression in Euclidean spaces [25], interpolation over manifolds [26], [16], Chapter 10 of [27], and ambient approximation over manifolds [28]. None of the recent studies of Koopman approximations [19], [20], [21], [22], [23] derive such rates of convergence in terms of fill distances.

(3) Rates of Convergence of the EDMD Algorithm Finally, this paper defines a general data-dependent approximation of the Koopman operator as it acts on a variety of function spaces. In some instances, this data dependent operator can be interpreted as a specific implementation of the extended dynamic mode decomposition (EDMD) algorithm. With this identification it is possible to derive rates of convergence for the EDMD algorithm in certain types of function spaces. This result is described in Theorem 3 and also has no precedent in the recent studies of the EDMD algorithm, as in [19], [22].

II. BACKGROUND THEORY

A. Symbols and Nomenclature

In this paper, \mathbb{R} is the set of the real numbers. We write $a \lesssim b$ to mean that there is a constant c that does not depend on a, b such that $a \leq cb$, and \gtrsim is defined similarly. We let $X = \mathbb{R}^d$ be the input space, and $Y := \mathbb{R}^n$ be the output space. We assume that Q is a smooth, compact Riemannian manifold that is regularly embedded in $X = \mathbb{R}^d$. The symbol $C(Q, Y)$ represents the space of continuous, Y -valued functions over the manifold Q , equipped with the usual supremum norm. We set $L_\mu^2(Q, Y)$ to be the usual Lebesgue space of Y -valued, μ -integrable functions over the manifold Q , with μ a measure on the manifold. This paper also employs the Sobolev space $W^{s,p}(Q)$ over the compact Riemannian manifold Q , which is defined intrinsically in [16] or extrinsically in [26]. Roughly speaking, for integer $s > 0$ this space consists of all functions in $L_\mu^p(Q)$ that have derivatives through order s that are elements of $L_\mu^p(Q)$. The Sobolev spaces for real smoothness parameter $s > 0$ are obtained as interpolation spaces from those that have integer order. [16] We write $\mathbb{W}^{s,p}(Q)$ for the Y -valued Sobolev spaces, $\mathbb{W}^{s,p}(Q) := (W^{s,p}(Q))^n$.

B. Reproducing Kernel Hilbert Spaces

A number of constructions in reproducing kernel Hilbert spaces are used in this paper, and the reader is referred to

[29], [30] for a good introduction that provides the needed background for the necessarily brief summary given here. Throughout the paper $\mathfrak{K} : X \times X \rightarrow \mathbb{R}$ will be an admissible kernel that defines a native space H of real-valued functions over X . We always assume that the kernel \mathfrak{K} is continuous, symmetric, and strictly positive definite in this paper, which means that for any finite set $\Xi_M := \{\xi_{M,i} \mid 1 \leq i \leq M\}$ of distinct points, the kernel matrix $[\mathfrak{K}(\xi_{M,i}, \xi_{M,j})] := \mathbb{K}(\Xi_M, \Xi_M) \in \mathbb{R}^{M \times M}$ is a positive definite matrix. Kernels of this type include the exponential kernel, inverse multi-quadric kernel, or Matern-Sobolev kernel, among others [27]. The space H is defined as $H := \overline{\text{span}\{\mathfrak{K}_x \mid x \in \Omega\}}$ where the closure is taken with respect to the inner product that is defined as $(\mathfrak{K}_x, \mathfrak{K}_y)_H = \mathfrak{K}(x, y)$ for all $x, y \in X$. The RKHS H is characterized by the fact that it satisfies the reproducing property: we have $(\mathfrak{K}_x, g)_H = g(x)$ for all $x \in X$ and $g \in H$.

In this paper, samples are generated along the trajectories of a discrete dynamical system over a subset $Q \subset X$ defined in terms of an unknown function f , and the function f defines an RKHS that is important for our analysis. For a mapping $f : Q \subset X \rightarrow X$, we define the pullback space $f^*(H)$ to be the set $\{h : Q \rightarrow \mathbb{R} \mid h = g \circ f, \text{ for some } g \in H\}$. The pullback space $f^*(H)$ is itself an RKHS, with its kernel $\mathfrak{K}^* : Q \times Q \rightarrow \mathbb{R}$ defined as $\mathfrak{K}^*(q_1, q_2) = \mathfrak{K}(f(q_1), f(q_2))$ for all $q_1, q_2 \in Q$. [30] The norm on the pullback space that is induced by the kernel \mathfrak{K}^* is equivalent to $\|h\|_{f^*(H)} := \inf\{\|g\|_H \mid h = g \circ f\}$. For a fixed $f : Q \rightarrow Q \subset X$ the Koopman operator U_f is defined as $U_f g = g \circ f$: this definition makes sense for scalar-valued functions $g \in H$ as well as vector-valued functions $g \in H^n$. We define the trace or restriction operator $Tg := g|_Q$. The space of restrictions $\mathcal{R} := T(H)$ is itself an RKHS space. It is induced by the kernel $\mathfrak{r} : Q \times Q \rightarrow \mathbb{R}$ that is the restriction of the kernel \mathfrak{K} , so that $\mathfrak{r}(x, y) := \mathfrak{K}(x, y)$ for all $x, y \in Q$. [29]

In this section, we review a few well-known observations regarding interpolation and projection for spaces defined in terms of scattered kernel bases. We summarize these properties for the finite-dimensional space $H_M := \text{span}\{\mathfrak{K}_{\xi_{M,i}} \mid \xi_{M,i} \in \Xi_M, 1 \leq i \leq M\}$ that is defined in terms of scattered bases in H that are located at the centers $\Xi_M := \{\xi_{M,1}, \dots, \xi_{M,M}\}$. We let $\Pi_M H \rightarrow H_M$ be the H -orthogonal projection onto the closed subspace $H_M \subset H$. Since we have assumed that the kernel \mathfrak{K} on H is strictly positive definite, we have the representation

$$\Pi_M g = \sum_{i,j=1}^M (\mathbb{K}(\Xi_M, \Xi_M))_{i,j}^{-1} g(\xi_{M,j}) \mathfrak{K}_{\xi_{M,i}}.$$

The projection operator Π_M induces the H -orthogonal decomposition $H = H_M \oplus Z_M$ where Z_M is the closed subspace $Z_M := \{f \in H \mid f(\xi) = 0 \text{ for all } \xi \in \Xi_M\}$. This decomposition implies that the complementary projection $I - \Pi_M$ satisfies $((I - \Pi_M)g)(\xi) = 0$ for all $\xi \in \Xi_M$. In other words, the orthogonal projection $\Pi_M g$ interpolates the function g at the points in Ξ_M . When studying the convergence properties of estimates over the set $Q \subset X$, it

is common that approximation errors are described in terms of the fill distance $h_{\Xi_M, Q}$ of the finite samples $\Xi_M \subset Q$ in the set Q . The fill distance is defined as $h_{\Xi_M, Q} = \sup_{q \in Q} \min_{\xi \in \Xi_M} d_Q(q, \xi)$ with d_Q the metric on Q .

The relationships among the H -orthogonal projection Π_M , the scattered bases $\mathfrak{K}_{\xi_{M,i}}$ in H_M , and the coordinate representation of Π_M , have been stated by considering H_M , a subset of the RKHS H induced by the kernel $\mathfrak{K} : X \times X \rightarrow \mathbb{R}$ of functions over the ambient space X . However, entirely analogous statements can be made for the projections onto finite-dimensional spaces \mathcal{R}_M and $f^*(H_M)$, which are defined simply by defining scattered bases in terms of the translates of the kernels $\mathfrak{r}_{\xi_{M,i}}$ and $\mathfrak{K}_{\xi_{M,i}}^*$, respectively, for $\xi_{M,i} \in \Xi_M$. To simplify notation in this paper, we use the generic operator Π_M to refer to any of the (generally different) projections from H, \mathcal{R} , or $f^*(H)$ onto H_M, \mathcal{R}_M , or $f^*(H_M)$, respectively. The specific choice of the domain and range of Π_M is clear from the context in any particular equation that follows.

C. Koopman Theory and EDMD Algorithm

We have noted earlier that the Koopman operator U_f is defined from the identity $U_f g := g \circ f$ for some fixed function f . One of the most common ways of approximating U_f is based on the extended dynamic mode decomposition (EDMD) algorithm. It has been studied carefully in recent work like [19], [20]. Here we summarize the EDMD method using nomenclature that is common in these references so that we can distinguish it from the data-driven approximation studied in this paper. From a set of input-output samples of Equation 1, we define two data matrices \mathbf{X} and \mathbf{Y} defined as follows,

$$\mathbf{X} = [x_1, \dots, x_M] \in \mathbb{R}^{d \times M},$$

$$\mathbf{Y} = [x_2, \dots, x_{M+1}] := f(\mathbf{X}) \in \mathbb{R}^{d \times M}.$$

We want to use these data matrices to construct estimates of the Koopman operator U_f . Since the operator U_f is infinite dimensional, we define a finite dimensional subspace for building approximations. Suppose we choose basis functions $\{\psi_i \mid 1 \leq i \leq M\}$ for our approximations. We introduce the vector $\psi = [\psi_1, \dots, \psi_M]^T$. With the definition of the basis functions in ψ , data matrices for the EDMD algorithm are then determined as follows

$$\Psi(\mathbf{X}) = [\psi(x_1), \dots, \psi(x_M)] \in \mathbb{R}^{N \times M},$$

$$\Psi(\mathbf{Y}) = [\psi(x_2), \dots, \psi(x_{M+1})] \in \mathbb{R}^{N \times M}.$$

Approximations of the Koopman operator U_f are constructed in terms of the matrix solution $A_{N,M} \in \mathbb{R}^{N \times N}$ of the minimization problem

$$A_{N,M} := \arg \min_{A \in \mathbb{R}^{N \times N}} \|A\Psi(\mathbf{X}) - \Psi(\mathbf{Y})\|_F^2$$

The solution of this minimization problem is given by $A_{N,M} = \Psi(\mathbf{Y}) (\Psi^T(\mathbf{X})\Psi(\mathbf{X}))^{-1} \Psi^T(\mathbf{X})$. Finally, the approximation $U_{N,M}$ of the Koopman operator U_f is given by

$$(U_{N,M}g)(\cdot) := \alpha^T A_{N,M} \psi(\cdot) \quad (3)$$

for any function $g(\cdot) := \alpha^T \psi(\cdot)$ with $\alpha \in \mathbb{R}^N$.

III. PROBLEM FORMULATION

The distribution-free learning problem is a general problem that has been studied in a wide variety of contexts, most commonly for mappings between Euclidean spaces. [25]. As in [12] we are interested in this paper in formulating and solving this problem, not over some known compact subset such as $\Omega := [a, b]^d \subset \mathbb{R}^d$, but rather over the unknown manifold Q .

A. Distribution-Free Learning in Euclidean Spaces

We begin by summarizing the general structure of the distribution-free learning problem for regression over $X := \mathbb{R}^d$, and subsequently, we discuss how the problem is cast in terms of the unknown manifold Q for certain types of discrete evolution laws. When the distribution-free learning problem is applied to regression, we are faced with building approximations of some unknown function over X that takes values in $Y = \mathbb{R}^n$. We are given samples $\{(x_{k_i}, y_{k_i})\}_{i=1}^M \subset X \times Y$. Here X is the inputs space and Y is the output space, and we can view the samples as perhaps noisy measurements of the functional relationship $y = G(x)$ where $G : X \rightarrow Y$ is unknown. As noted previously, it is usually assumed that the samples are independent and identically distributed, with ν the probability distribution over $X \times Y$ that generates the samples. In the distribution-free learning problem, the probability distribution ν is unknown. The aim of learning theory is to build an approximation of the unknown function using the samples that makes some error measure small, and here we use the familiar quadratic error for arbitrary functions $g : X \rightarrow Y$,

$$E_\mu(g) := \int_X \int_Y \|y - g(x)\|_Y^2 \nu(dx, dy), \quad (4)$$

where again we interpret $y = G(x)$ in the ideal case. A great deal is known about the structure of this particular problem in the space $L_\mu^2(\mathbb{R}^d)$, or even in $L_\mu^2(\Omega)$ with Ω a nice compact subset of X like $\Omega = [a, b]^d$. It is known that the minimization of the quadratic error E_μ above is equivalent to minimizing the expression

$$E_\mu(g) := \int_X \|g(x) - H_\mu(x)\|_Y^2 \mu(x) + E_\mu(H_\mu) \quad (5)$$

where the measure ν is written as $\nu(dx, dy) = \mu_x(dy)\mu(dx)$, $\mu_x(dy)$ is the conditional probability over Y given $x \in X$, $\mu(dx)$ is the marginal measure of ν over X , and $H_\mu(x) := \int_Y y \mu_x(dy)$ is the regressor function. Thus, the regressor H_μ is the optimal minimizer, but it cannot be computed from this closed form expression since ν , and therefore μ_x is unknown. In practice, then, the ideal error measure above is replaced with the discrete

$$E_M(g) := \frac{1}{M} \sum_{i=1}^M \|y_i - g(x_i)\|_Y^2 \quad (6)$$

that depends on the samples $\{(x_i, y_i)\}_{i=1}^M$, which leads to the method of empirical risk minimization. (Traditionally, note that the minimization is over sequentially collected samples in Equation 6.) Note that the discrete error above can be evaluated for any given g . When estimates $G_{M,N} =$

$\arg \inf \{E_M(g) \mid g \in H_N\}$ that minimize the empirical risk are calculated for some N dimensional space H_N of approximants, it is then possible to address in what sense $G_{M,N} \rightarrow G_\mu$ as the number of samples M and the dimension N approach ∞ . The theory for such approximations is mature, and a summary of the state art in these cases can be found [25], [31], [32].

B. Distribution-Free Learning over an Unknown Manifold

The manifold estimation problem studied in this paper modifies the classical learning problem above in a number of ways: some changes are minor, while others lead to subtle issues. Note carefully that the samples generated by Equations 1 are defined from a deterministic, nonlinear, dependent measurement process, not one that is IID. It turns out that the assumption that samples are IID is central to many of the most refined estimates of errors in distribution-free learning theory. We will analyze the system in Equation 1 in two ways in this and the next few sections. In this section, we assume that the samples $\{(x_i, y_i)\}_{i=1}^M$ are generated by choosing initial conditions randomly according to the unknown measure μ on Q , and then observations y_i are defined as in Equation 2. That is, the samples $\{(x_i, y_i)\}_{i=1}^M$ are understood as the initial condition responses of the system in Equations 1 and 2 as the initial condition is chosen randomly over the unknown manifold Q . (Later we extend our analysis to the case when samples are dependent and determined along a trajectory.) In this case, the measure ν that generates the samples has the particular form $\nu(dx, dy) = \delta_{G(f(x))}(dy)\mu(dx)$, and the regressor function is $H_\mu(x) := \int_Y y \delta_{G(f(x))}(dy) = G \circ f$. With these definitions, the ideal error E_μ in Equations 4 and 5 makes sense for the Lebesgue space of functions $L_\mu^2(Q, Y)$ defined over the manifold Q without change. Likewise, the empirical error E_M in Equation 6 makes sense, since the evaluation operator is well-defined on $H \subset C(X)$. In this situation, in contrast to the form of the regression error functional in Equation 5, we consider the ideal error

$$E_\mu(g) = \int_Q \|(U_f(g - G))(x)\|_Y^2 \mu(dx) + E_\mu(U_f G),$$

where $U_f h = h \circ f$ is the Koopman operator induced by the unknown function f that defines the unknown dynamics. The corresponding discrete error function is then

$$\begin{aligned} E_M(g) &:= \frac{1}{M} \sum_{i=1}^M \|y_i - (g \circ f)(x_i)\|_Y^2 = \frac{1}{M} \sum_{i=1}^M E_i^k(g), \\ &= \frac{1}{M} \sum_{k=1}^n \sum_{i=1}^M |(G^k \circ f)(x_i) - (g^k \circ f)(x_i)|^2, \end{aligned}$$

where we have introduced the component-wise notation $g := (g^1, \dots, g^n)$ and $G := (G^1, \dots, G^n)$.

C. Projection for Regression in the Pullback Space

We start with a straightforward analysis under the assumptions of the last Section III-B. We interpret the empirical risk minimization in terms of projection or interpolation in a pullback space. We have chosen to start with this

elementary case, since it makes clear some of the issues that distinguish the learning problem in this paper from the usual one in Euclidean space. We consider the minimization $g_M^k := \operatorname{argmin}\{E_M^k(g^k) \mid g^k \in H_M\}$ with $H_M := \operatorname{span}\{\mathcal{K}_{\xi_{M,i}} \mid \xi_{M,i} \in \Xi_M\}$ that defines the empirical risk minimizer.

Theorem 1: Suppose that $f(\Xi_M) := \{f(\xi_{M,i}) \mid \xi_{M,i} \in \Xi_M\}$ are distinct points. The empirical risk minimizer g_M^k satisfies

$$(U_f g_M^k(\cdot)) := \sum_{i,j}^M (\mathbb{K}(f(\Xi_M), f(\Xi_M)))_{i,j}^{-1} y_j^k \mathcal{K}(f(x_i), f(\cdot)) \quad (7)$$

Proof: The proof of this theorem is a direct consequence of scattered data interpolation over the pullback space $f^*(H)$. Define the space of approximants

$$H_M^* := \operatorname{span}\{\mathcal{K}_{\xi_{M,i}}^* \mid \xi_{M,i} \in \Xi_M\} \subset f^*(H).$$

In this case, if we obtain a solution $h_M^k \in f^*(H)$ to a minimization problem over the pullback space $f^*(H)$,

$$h_M^k = \operatorname{argmin}_{h \in f^*(H)} \frac{1}{M} \sum_{i=1}^M |(y_i^k - h)(x_i)|^2, \quad (8)$$

then, for any function $g_M^k \in H$ such that $h_M^k = U_f g_M^k$, g_M^k solves the empirical risk minimization problem in Equation 7. But Equation 8 is solved by the function $h_M^k \in f^*(H)$ that interpolates the samples $\{(x_i, y_i^k)\}_{i=1}^M$, since in this case the right hand side of Equation 8 is precisely zero. The right hand side of Equation 4 is precisely the coordinate expression for the $f^*(H)$ -orthogonal projection onto $H_M^* := f^*(H_M)$. Since the kernel \mathcal{K} is assumed to be positive definite over $X \times X$, it follows that the pullback kernel $\mathcal{K}^*(\cdot, \cdot) = \mathcal{K}(f(\cdot), f(\cdot))$ is also strictly positive definite over $Q \times Q$. The assumption that $f(\Xi)$ are distinct points ensures that the Grammian in Equation 7 is invertible. ■

Overall, Theorem 1 is quite informative. It shows that the distribution-free learning problem at hand, which is expressed in terms of an unknown manifold Q , measures μ on Q , and function $f : Q \rightarrow Q$, can in principle be solved as a simple regression problem on the pullback space $f^*(H)$. Unfortunately, the solution in Equation 7 is not of practical use in the problem at hand, since the solution depends on the unknown function f . This makes clear a point that distinguishes the learning problem on manifolds that we study here, where the dynamics propagates according to some unknown function f , from the classical regression problem.

D. Data-Driven Approximations

Finally, we study the uncertain system in Equations 1 and 2 in its full generality. The samples $\{(x_{k_i}, y_{k_i})\}_{i=1}^M$ are collected along the deterministic, nonlinear system at discrete times $\mathbb{T}_M := \{k_i \mid 1 \leq i \leq M\}$. Now the measure μ is taken to be some convenient probability measure over Q for defining average error, but it does not generate the samples randomly. In this section we define a data-driven

approximation U_f^M of the Koopman operator, which is used to bound the excess risk, which is defined by the left hand side of the inequality

$$\begin{aligned} E_\mu(g) - E_\mu(U_f G) &= \int_Q \|(U_f(G - g))(x)\|_Y^2 \mu(dx), \\ &\lesssim \left(\max_{1 \leq k \leq n} \|U_f(G^k) - U_f(g^k)\|_{C(Q, \mathbb{R})} \right)^2. \end{aligned}$$

We make the structural assumption that the pullback space $f^*(H)$ of functions over the manifold Q is continuously embedded in the space of restrictions $\mathcal{R} := T(H)$, $f^*(H) \hookrightarrow \mathcal{R}$, and furthermore, that the space of restrictions \mathbb{R} is embedded continuously in the Sobolev space $W^{t,2}(Q)$. Following the strategy in [33], we define the data dependent approximation $U_f^M g$ of $U_f g$ to be given by

$$U_f^M g := \Pi_M((\Pi_M g) \circ f),$$

where this equation is interpreted componentwise for the vector-valued function g . That is, $U_f^M g := (U_f^M g^1, \dots, U_f^M g^n)$ for $g = (g^1, \dots, g^n)$. Based on the discussion in Section II-B, the coordinate expression for each component of this operator is

$$\begin{aligned} U_f^M g^k &:= \sum_{i,j=1}^M (\mathbb{K}(\Xi_M, \Xi_M))_{i,j}^{-1} \\ &\times \sum_{p,q=1}^M (\mathbb{K}(\Xi_M, \Xi_M))_{p,q}^{-1} g^k(\xi_{M,q}) \mathbb{K}(\Xi_M, f(\Xi_M))_{p,j} \mathfrak{K}_{\xi_{M,i}}. \end{aligned} \quad (9)$$

Theorem 2: Suppose that $f^*(H) \hookrightarrow \mathcal{R} \approx W^{t,2}(Q)$. Then there are constants $C, H > 0$ such that for all $\Xi_M \subset Q$ that satisfy $h_{\Xi_M, Q} \leq H$, we have

$$\|(U_f G)(x) - (U_f^M G)(x)\|_Y \leq C h_{\Xi_M, Q}^{t-m} \|g\|_{W^{t,2}(Q)}$$

for all $g \in W^{t,2}(Q)$ and $x \in Q$.

Proof: We define the approximation $U_f^M G$ as above, $U_f^M G = \Pi_M((\Pi_M G) \circ f)$. Note that the coordinate expression for $U_f^M G$ can be calculated using the observations $\{(x_i, y_i)\}_{i=1}^M = \{(x_i, G(f(x_i)))\}_{i=1}^M$. (Here we assume that we have collected the one additional measurement $x_{M+1} = f(x_M)$ also that is needed in the coordinate expression.) The proof of this theorem follows that strategy in [33], generalizing it to the case when $Y = \mathbb{R}^n$, where

$$\begin{aligned} &\|(U_f G)(x) - (U_f^M G)(x)\|_Y \\ &\lesssim \max_{1 \leq k \leq n} |(G^k \circ f)(x) - \Pi_M((\Pi_M G^k) \circ f)|, \\ &\leq \max_{1 \leq k \leq n} \left\{ \underbrace{\|(I - \Pi_M)G^k\|_{C(Q, \mathbb{R})}}_{\text{term 1}} + \right. \\ &\quad \left. + \underbrace{\|(I - \Pi_M)((\Pi_M G^k) \circ f)\|_{C(Q, \mathbb{R})}}_{\text{term 2}} \right\}. \end{aligned}$$

Both term 1 and term 2 above are bounded using the many zeros Theorem 4 on the manifold Q . Term 1 is bounded using

the fact that $\mathcal{R} \approx W^{t,2}(Q) \hookrightarrow W^{m,2}(Q)$ and subsequently

$$\begin{aligned} \|(I - \Pi_M)G^k\|_{C(Q, \mathbb{R})} &\lesssim \|(I - \Pi_M)G^k\|_{W^{m,2}(Q)}, \\ &\lesssim h_{\Xi_M, Q}^{t-m} \|(I - \Pi_M)G^k\|_{W^{t,2}(Q)}, \\ &\lesssim h_{\Xi_M, Q}^{t-m} \|G^k\|_{W^{t,2}(Q)}. \end{aligned}$$

In the above we have applied Theorem 4 to the term $(I - \Pi_M)G^k$, which vanishes on Ξ_M . We also use that fact that Π_M is a bounded operator on $\mathcal{R} = W^{t,2}(Q)$. We can similarly bound the second term: (term 2) $\lesssim h_{\Xi_M, Q}^{t-m} \|U_f \Pi_M G^k\|_{W^{t,2}(Q)}$. By virtue of the assumption that $f^*(H) \hookrightarrow \mathcal{R} \approx W^{t,2}(Q)$, we know (term 2) $\lesssim h_{\Xi_M, Q}^{t-m} \|G^k\|_{W^{t,2}(Q)}$ also. Collecting the different inequalities for each of the components $1 \leq k \leq n$ finishes the proof. ■

We close this section by showing that the analysis of this section enables similar error bounds to be defined for certain cases of the EDMD algorithm.

Theorem 3: Suppose that $U_{M,M}$ is the approximation of the Koopman operator derived by the EDMD algorithm in Equation 3 using the samples $\{(x_{k_i}, y_{k_i})\}_{i=1}^M$, so that the basis vector ψ is selected as $\psi := \{\mathfrak{K}_{x_{k_1}}, \dots, \mathfrak{K}_{x_{k_M}}\}^T$. Under the hypotheses of Theorem 2, we have

$$\|(U_f G)(x) - (U_{M,M} G)(x)\|_Y \leq C h_{\Xi_M, Q}^{t-m} \|g\|_{W^{t,2}(Q)}$$

for the EDMD approximation $U_{M,M}$ of the Koopman operator U_f .

Proof: In general, the EDMD approximation of the Koopman operator depends on two parameters, the number of samples M and the number of basis functions N . It is a more general method of building an approximation of U_f than U_f^M in this paper. However, when $M = N$ and the basis vector ψ consists of $\psi := \{\mathfrak{K}_{\xi_1}, \dots, \mathfrak{K}_{\xi_M}\}^T$, then the coordinate expression in Equation 9 for U_f^M is precisely the same as that in Equation 3. Since $U_f^M = U_{M,M}$, the error bound follows. ■

IV. NUMERICAL RESULTS AND CONCLUSIONS

This section summarizes numerical results for some examples of estimates given a family of observations $\{(x_i, y_i)\}_{i=1}^M$ collected over an unknown manifold Q . We set the centers $\Xi_M := \{x_1, \dots, x_M\}$ in this section. For our first example, we consider a simple closed form case to illustrate the concepts behind our empirical estimate. Our evolution $f : Q \rightarrow Q$ corresponds to the dynamics of a pendulum following the Störmer-Verlet scheme as given in Example 1.4 in [34]. In this example, X_1 and X_2 correspond to the pendulum's momentum and position respectively. We build estimates for an unknown function $G : X := \mathbb{R}^2 \rightarrow \mathbb{R}$ from samples collected over $Q = \subset \mathbb{R}^2$. The function G is defined for each $x := \{x_1, x_2\} \in \mathbb{R}^2$ by $G(x) = 1.5 - \sin(x_2) + \frac{1}{9}x_1^2$. Figure 1 depicts the estimates of the Koopman operator acting on the observable function G . In these studies, we use the Matern-Sobolev kernel,

$$\mathfrak{K}(\xi_{M,j}, x) = \left(1 + \frac{\sqrt{3}\|x - \xi_{M,j}\|_2^2}{\beta} \right) e^{-\left(\frac{\sqrt{3}\|x - \xi_{M,j}\|_2^2}{\beta} \right)}$$

with $\|\cdot\|$ as the standard Euclidean metric over \mathbb{R}^2 and the hyperparameter $\beta = 0.15$. From the figure, it is evident that

the approximation closely matches the intersection between the true function surface $U_f G$ and the surface generated from the RKHS basis, $U_f^M G$. This is a result of the interpolating properties of the RKHS approximation.

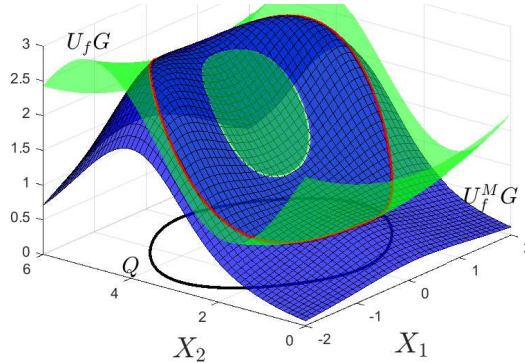


Fig. 1. An example of the $U_f G$ approximation in green of G , represented by the light yellow surface. Using M samples collected over the composition $U_f G$ the finite dimensional approximation $U_f^M G$ is generated from the RKHS represented by the mesh blue surface. Minimizing the empirical risk over the samples corresponds to interpolating the function over the samples as represented by the red dashed line.

Figure 2 demonstrates the calculated error convergence of the estimate of the Koopman approximation to the true function as the number of samples increased. An increase in the number of samples collected on the manifold reduces the fill distance that bounds the error of the approximation. The decay rate is determined by selecting t and m as described in [33]. From the figure, it is clear that the error is bounded by $\mathcal{O}(h_{\Xi_M}^{t-m})$, which is represented by the dashed line above the curve.

Our second example uses three-dimensional motion capture data collected in [35] during a human walking experiment on a treadmill. The experiment tracks 5000 marker coordinates relative to a fixed inertial frame defined by the camera's fixed position. For this simulation, a small candidate kinematic model is defined from the full collection of experimental trajectories. The marker coordinates of the hip, knee, and ankle in the full data set are projected to the sagittal plane that divides the left and right half of the body see Figure 3. With this projection, the joint angle θ_1 roughly corresponds to hip flexion. It is calculated from the projected vector v_1 that connects the hip to knee from the inertial b_1 vector in the plane. The knee flexion angle θ_2 is calculated by taking the dot product between the vector v_1 and the vector connecting the knee to the ankle v_2 in the sagittal plane. We then take these joint angles of the left leg as defining our configuration manifold Q . The measured outputs corresponded to the marker positions themselves and could be of arbitrary dimension n . For illustrative purposes, we chose to examine the kinematic map from the joint angles θ_1 and θ_2 to the ankle coordinate associated with the b_2 vector. Figure 4 shows the estimate of part of the forward kinematics from the empirical risk minimizer using 64 samples and kernel functions. Note that the estimate can be extended to observables $n > 1$ such as the ankles coordinates that

correspond to the b_1, b_2 , and b_3 vectors, but we would not be able to visualize all such coordinates simultaneously in the estimate.

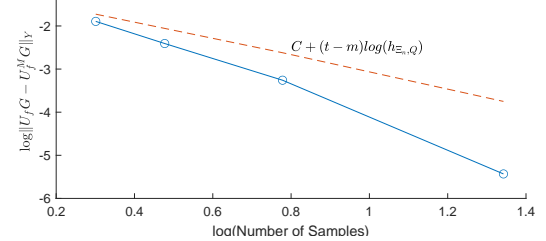


Fig. 2. The rate of convergence of the estimate of the Koopman approximation. The rate of convergence is bounded by the fill distance represented by the dashed line above the curve.

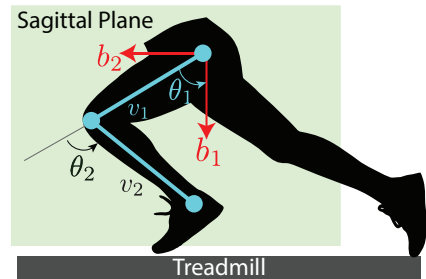


Fig. 3. An illustration of the inputs θ_1 and θ_2 , which roughly correspond to hip and knee flexion. These input variables can be mapped to measured marker coordinates placed on joints such as the knee or ankle.

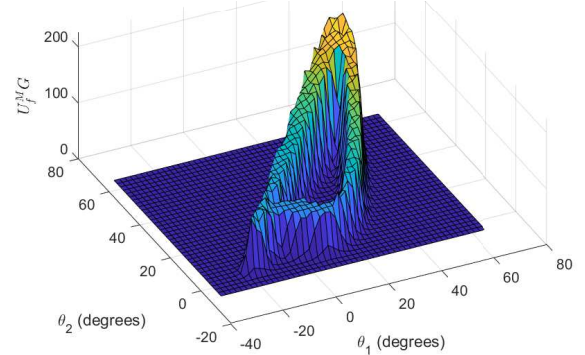


Fig. 4. The estimate of our b_2 -coordinate of the marker positioned on the left ankle using inputs θ_1 and θ_2 .

V. CONCLUSION

This paper has derived methods for estimation of animal motions. We have derived a closed form expression for the empirical risk minimizer in a pullback RKHS space that depends on the unknown dynamics. We also have shown that approximations of the unknown function $G : Q \rightarrow Y$ can be constructed in terms of a data-dependent approximation of the the Koopman operator. For the kernel based method, we have derived error bounds based on scattered samples and kernel dependent bases defined over Q . Finally, we have presented numerical results to better illustrate the qualitative behavior of the algorithms.

APPENDIX

The proof of convergence for the approximation of the Koopman operator in Section III-D uses a version of the many zeros theorem that holds over compact, smooth, regularly embedded submanifolds $S \subset \mathbb{R}^d$.

Theorem 4 ([26] Lemma 10): Let Q be a k dimensional smooth manifold, $t \in \mathbb{R}$ with $t > k/2$, and $m \in \mathbb{N}$ satisfy $0 \leq m \leq \lceil t \rceil - 1$. There there are constants C, H such that if $h_{\Xi_M, Q} \leq H$ and $f \in W^{t,2}(Q)$ satisfies $f|_{\Xi_M} = 0$, then

$$|f|_{W^{m,2}(Q)} \leq Ch_{\Xi_M}^{t-m} |f|_{W^{t,2}(Q)}.$$

To apply this theorem in applications, we will need to choose the kernel $\hat{\mathcal{K}}$ that is defined on all of X in such a way that the space of restrictions \mathcal{R} to Q is equivalent to a Sobolev space over Q . This can be achieved using the strategy outline on page 1759 of [26]. The kernel $\hat{\mathcal{K}}$ on $X \times X$ is said to have algebraic decay if its Fourier transform $\hat{\mathcal{K}}$ has algebraic decay in the sense that $\hat{\mathcal{K}}(\xi) \sim (1 + \|\xi\|_2^2)^{-\tau}$ for $\tau > d/2$. If the kernel satisfies this algebraic decay condition, then it follows that $H = W^{\tau,2}(\mathbb{R}^d)$. We then can use the following theorem, again from [26].

Theorem 5 ([26] Theorem 5): If the kernel $\hat{\mathcal{K}}$ that induces H satisfies the algebraic growth condition with exponent τ , then we have $\mathcal{R} = T(H) = W^{\tau-(d-k)/2,2}(Q)$.

REFERENCES

- [1] Aleksandra V. Birn-Jeffery and Timothy E. Higham. Geckos decouple fore- and hind limb kinematics in response to changes in incline. *Frontiers in Zoology*, 13(1):1–13, 2016.
- [2] Rivers Ingersoll, Lukas Haizmann, and David Lentink. Biomechanics of hover performance in Neotropical hummingbirds versus bats. *Science Advances*, 4(9):eaat2980, 2018.
- [3] Laura B Porro, Amber J Collings, Enrico A Eberhard, Kyle P Chadwick, and Christopher T Richards. Inverse dynamic modelling of jumping in the red-legged running frog, *kassina maculata*. *Journal of Experimental Biology*, 220(10):1882–1893, 2017.
- [4] Jeffrey Aguilar, Tingnan Zhang, Feifei Qian, Mark Kingsbury, Benjamin McInroe, Nicole Mazouchova, Chen Li, Ryan Maladen, Chaohui Gong, Matt Travers, et al. A review on locomotion robophysics: the study of movement at the intersection of robotics, soft matter and dynamical systems. *Reports on Progress in Physics*, 79(11):110001, 2016.
- [5] Giovanna Catavitello, Yury Ivanenko, and Francesco Lacquaniti. A kinematic synergy for terrestrial locomotion shared by mammals and birds. *Elife*, 7:e38190, 2018.
- [6] Matthew Brand and Aaron Hertzmann. Style machines. In *Proceedings of the 27th annual conference on Computer graphics and interactive techniques*, pages 183–192, 2000.
- [7] Jack M Wang, David J Fleet, and Aaron Hertzmann. Gaussian process dynamical models for human motion. *IEEE Transactions on Pattern Analysis and Machine Intelligence*, 30(2):283–298, 2007.
- [8] Judith Butepage, Michael J Black, Danica Kragic, and Hedvig Kjellstrom. Deep representation learning for human motion prediction and classification. In *Proceedings of the IEEE conference on computer vision and pattern recognition*, pages 6158–6166, 2017.
- [9] Ashesh Jain, Amir R Zamir, Silvio Savarese, and Ashutosh Saxena. Structural-rnn: Deep learning on spatio-temporal graphs. In *Proceedings of the ieee conference on computer vision and pattern recognition*, pages 5308–5317, 2016.
- [10] Katerina Fragkiadaki, Sergey Levine, Panna Felsen, and Jitendra Malik. Recurrent network models for human dynamics. In *Proceedings of the IEEE International Conference on Computer Vision*, pages 4346–4354, 2015.
- [11] Zimo Li, Yi Zhou, Shuangjiu Xiao, Chong He, Zeng Huang, and Hao Li. Auto-conditioned recurrent networks for extended complex human motion synthesis. *arXiv preprint arXiv:1707.05363*, 2017.
- [12] Nathan Powell and Andrew J Kurdila. Learning theory for estimation of animal motion submanifolds. In *2020 59th IEEE Conference on Decision and Control (CDC)*, pages 4941–4946. IEEE, 2020.
- [13] Francesco Bullo and Andrew D. Lewis. *Geometric Control of Mechanical Systems*, volume 49 of *Texts in Applied Mathematics*. Springer Verlag, New York-Heidelberg-Berlin, 2004.
- [14] Kevin M Lynch and Frank C Park. *Modern Robotics*. Cambridge University Press, 2017.
- [15] Thomas Hangelbroek and Dominik Schmid. Surface spline approximation on $so(3)$. *Applied and Computational Harmonic Analysis*, 31(2):169–184, 2011.
- [16] Thomas Hangelbroek, Francis J Narcowich, and Joseph D Ward. Polyharmonic and related kernels on manifolds: interpolation and approximation. *Foundations of Computational Mathematics*, 12(5):625–670, 2012.
- [17] Steven L Brunton, Marko Budišić, Eurika Kaiser, and J Nathan Kutz. Modern koopman theory for dynamical systems. *arXiv preprint arXiv:2102.12086*, 2021.
- [18] Alexandre Mauroy, Igor Mezić, and Yoshihiko Susuki. *The Koopman Operator in Systems and Control: Concepts, Methodologies, and Applications*. Springer, 2020.
- [19] Stefan Klus, Peter Koltai, and Christof Schütte. On the numerical approximation of the perron-frobenius and koopman operator. *Journal of Computational Dynamics*, 3(1):51–77, 2016.
- [20] Milan Korda and Igor Mezić. On convergence of extended dynamic mode decomposition to the koopman operator. *Journal of Nonlinear Science*, 28(2):687–710, 2018.
- [21] Romeo Alexander and Dimitrios Giannakis. Operator-theoretic framework for forecasting nonlinear time series with kernel analog techniques. *Physica D: Nonlinear Phenomena*, 409:132520, 2020.
- [22] Igor Mezić. On numerical approximations of the koopman operator. *arXiv preprint arXiv:2009.05883v1 [math.DS]*, 2020.
- [23] Stefan Klus, Feliks Nuske, Sebastian Peitz, Jan-Hendrik Niemann, Cecilia Clementi, and Christof Schütte. Data-Driven Approximation of the Koopman Operator: Model Reduction System Identification, and Control. *Physica D: Nonlinear Phenomena*, 406, May 2020.
- [24] Marko Budišić, Ryan Mohr, and Igor Mezić. Applied Koopmanism. *Chaos: An Interdisciplinary Journal of Nonlinear Science*, 22(4):047510, 2012.
- [25] László Györfi, Michael Kohler, Adam Krzyzak, and Harro Walk. *A Distribution-free Theory of Nonparametric Regression*. Springer Science & Business Media, 2006.
- [26] Edward Fuselier and Grady B. Wright. Scattered data interpolation on embedded submanifolds with restricted positive definite kernels: Sobolev error estimates. *SIAM J. Numer. Anal.*, 50(3):1753–1776, 2012.
- [27] Holger Wendland. *Scattered Data Approximation*, volume 17. Cambridge university press, 2004.
- [28] Lars-Benjamin Maier. *Ambient Approximation of Functions and Functionals on Embedded Submanifolds*. PhD thesis, Technischen Universität Darmstadt, 2018.
- [29] Alain Berlinet and Christine Thomas-Agnan. *Reproducing Kernel Hilbert spaces in Probability and Statistics*. Springer Science & Business Media, 2011.
- [30] Saburo Saitoh, Daniel Alpay, Joseph A Ball, and Takeo Ohsawa. *Reproducing Kernels and Their Applications*, volume 3. Springer Science & Business Media, 2013.
- [31] Ronald DeVore, Gerard Kerkyacharian, Dominique Picard, and Vladimir Temlyakov. Mathematical methods for supervised learning. *IMI Preprints*, 22:1–51, 2004.
- [32] Ronald DeVore, Gerard Kerkyacharian, Dominique Picard, and Vladimir Temlyakov. Approximation methods for supervised learning. *Foundations of Computational Mathematics*, 6(1):3–58, 2006.
- [33] S. T. Paruchuri, J. Guo, M. Kepler, T. Ryan, H. Wang, A. J. Kurdila, and D. Stilwell. Intrinsic and extrinsic approximation of koopman operators over manifolds. In *2020 59th IEEE Conference on Decision and Control (CDC)*, pages 1608–1613, 2020.
- [34] Ernst Hairer, Marlis Hochbruck, Arieh Iserles, and Christian Lubich. Geometric numerical integration. *Oberwolfach Reports*, 3(1):805–882, 2006.
- [35] Claudiane A Fukuchi, Reginaldo K Fukuchi, and Marcos Duarte. A public dataset of overground and treadmill walking kinematics and kinetics in healthy individuals. *PeerJ*, 6:e4640, 2018.